Philosophical Magazine, 21 December 2003
Vol. 83, No. 36, 4103–4122

Structure of dislocations and stacking faults in the complex intermetallic ξ'-(Al–Pd–Mn) phase

H. Klein†

Laboratoire de Cristallographie, 25 avenue des Martyrs, 38042 Grenoble Cedex 9, France

and M. Feuerbacher

Institut für Festkörperforschung, Forschungszentrum Jülich GmbH, D-52425 Jülich, Germany

[*Received 31 January 2003 and accepted in revised form 7 August 2003*]

Abstract

We present the results of an electron microscopy study of defects in plastically deformed single crystals of the intermetallic ξ'-(Al–Pd–Mn) phase. Pure edge dislocations with two different Burgers vector directions and four different Burgers vector magnitudes were found. All Burgers vector magnitudes observed can be described in terms of irrational fractions of the unit-cell parameters, and we have observed Burgers vector directions that can be indexed using irrational indices. The stacking faults observed have displacement vectors whose magnitudes and directions are incompatible with the unit cell of the ξ' phase. A comparison of the Burgers vectors observed in this study with those reported for the corresponding icosahedral quasicrystal shows that they are equivalent with respect to their directions and lengths. This leads to the conclusion that local order rather than long-range periodic (or quasiperiodic) order governs the structure of defects in these materials.

§ 1. Introduction

The microstructural mechanisms of plastic deformation in intermetallic phases have been studied so far either in rather simple structures, for example Ni_3Al (Yamaguchi and Umakoshi 1990) (see also Sauthoff (1995)), or in the highly complex and not yet fully understood structures of quasicrystals (Feuerbacher *et al*. 1997). For both types of phase it has been shown that plastic shear is achieved by dislocation motion (Hirth and Lothe 1968, Wollgarten *et al*. 1993). This was rather surprising for the case of quasicrystals because of their non-periodic structure.

It is therefore reasonable to assume that, in an intermetallic phase with a large unit cell, plastic deformation is mediated by a dislocation mechanism as well. However, in this case a perfect dislocation would require a large Burgers vector magnitude which would lead to an unfavourably high line energy (Hirth and Lothe 1968). Splitting of the perfect dislocation into partials could possibly lower

† Email: holger.klein@grenoble.cnrs.fr.

Philosophical Magazine ISSN 1478–6435 print/ISSN 1478–6443 online
http://www.tandf.co.uk/journals
DOI: 10.1080/14786430310001613200

the line energy, but only at the expense of the introduction of a stacking fault between them. Recently we showed that such a mechanism does not operate in the case of the large-unit-cell intermetallic phase ξ'-(Al–Pd–Mn) (Klein *et al.* 1999). In this material the Burgers vector magnitudes of the dislocations observed were found to amount to only a small irrational fraction of the unit-cell parameter *without* incorporation of a stacking fault. It has been shown that the dislocation is accommodated into the structure by the introduction of a novel type of defect termed a phason line (cf. § 2).

Considerable work has been devoted to the description of quasicrystals and their defects during the last decade. Quasicrystal structures can, despite their lack of translational symmetry, be closely described in terms of a cubic hyperlattice in a higher-dimensional space (Janot 1992). This higher-dimensional crystallography approach is also used for the description of dislocations and their strain fields (Bohsung and Trebin 1989, Wollgarten *et al.* 1991, Kléman 1995). For icosahedral quasicrystals, the use of a six-dimensional (6D) hyperspace is required. Consequently, dislocation Burgers vectors in icosahedral phases are 6D vectors, which can be subdivided into two three-dimensional components. The physical-space component, termed the phonon part, describes the elastic lattice distortion due to the presence of the dislocation line and corresponds to the Burgers vector of dislocations in periodic crystals. The phason part, representing the strain components in an orthogonal complementary space, refers to the phason defects attributed to the dislocation. Phason defects are local rearrangements of atoms leading to a departure from the ideal quasiperiodic order (for example Janot (1992)). These defects can also be understood as matching-rule violations in a tiling description of the quasicrystal lattice.

In this paper we present the observation of dislocations in the ξ' phase. Different Burgers vector directions and magnitudes were observed. The Burgers vector magnitudes are shown to amount to irrational fractions of the unit-cell parameters and to follow a geometrical sequence equivalent to that observed for Burgers vectors in icosahedral Al–Pd–Mn (Rosenfeld *et al.* 1995, Feuerbacher *et al.* 1997). The relations between the Burgers vectors in the ξ' phase and the related icosahedral quasicrystal are discussed. Furthermore, we report the observation of stacking faults and the interactions between different defects in ξ'-(Al–Pd–Mn).

§ 2. Experimental details

Single crystals of the ξ'-(Al–Pd–Mn) phase obtained by Bridgman and Czochralski techniques (Feuerbacher *et al.* 2003) were deformed at a high temperature in three-point bending (Klein *et al.* 2000) and uniaxial compression geometries (Feuerbacher *et al.* 2001). In each case the orientation of the crystallographic axes of the sample with respect to the deformation geometry was chosen such that the creation and motion of dislocations with line directions parallel to [010] were favoured. Transmission electron microscopy (TEM) specimens were prepared by subsequent grinding, polishing and argon-ion milling. Our observations have been made using JEOL 4000EX and PHILIPS CM 20FEG transmission electron microscopes operated at 400 and 200 kV respectively. We have imaged the dislocations at specimen orientations parallel to the [010] direction overfocused by about 30 nm and with an objective-lens aperture selecting a symmetrical arrangement of beams. Under these conditions, the TEM images are comparable with corresponding tiling descriptions and therefore allow for direct conclusions on the structure of defects.

§ 3. Recall of the structure and phason defects of the ξ′-(Al–Pd–Mn) phase

The stoichiometric composition of the ξ′-(Al–Pd–Mn) phase is about $Al_{74}Pd_{22}Mn_4$. It has an orthorhombic structure of space group *Pnma* (Boudard *et al.* 1996). The unit cell, which contains 320 atoms, has cell parameters $a = 23.541$ Å, $b = 16.566$ Å and $c = 12.339$ Å.

Figure 1 (*a*) shows a TEM image taken along the [010] axis of the perfect structure. The bright-dot contrast is ordered in a pattern of flattened hexagons of edge length 7.76 Å, which are arranged in rows of alternating orientations (white lines in figure 1 (*a*)). In figure 1 (*b*) a schematic tiling representation of the ideal structure of the ξ′ phase in terms of flattened hexagons is shown. A comparison with the atomic structure of the ξ′ phase (Boudard *et al.* 1996) by means of TEM image simulations using the EMS program package (Stadelmann 1987) shows that the bright-contrast dots correspond to projections of columns of Mackay-type clusters. These clusters consist of concentric shells of icosahedral symmetry and consist of about 52 atoms. The distance between the centres of neighbouring clusters is equal to the edge length of the flattened hexagons. The clusters overlap slightly, sharing several atoms, which leads to specific 'bond' angles of 108° and 144°, the angles observed in the flattened hexagons. A comparison with the icosahedral phase $Al_{70.5}Pd_{21.0}Mn_{8.5}$ (Boudard *et al.* 1992) shows the existence of the same clusters in this phase. Moreover, they show the same centre-to-centre distance and 'bond' angles. The observation of intergrown ξ′ and icosahedral phases has shown that the [001] axis of the ξ′ phase is parallel to a twofold axis of the icosahedral phase and that the [010] axis is parallel to a fivefold axis of the quasicrystal (Klein *et al.* 1996).

A novel type of linear defect has been observed in the ξ′ structure by Klein *et al.* (1996). In projection, seen along the [010] direction, it can be represented by a banana-shaped polygon and an attached regular pentagon within the tiling of flattened hexagons (labelled A in figure 2). The line direction of this type of defect is always parallel to the [010] axis and it can move parallel to the [001] direction. The line can contain kinks along its direction of movement, resulting in the tiling representation labelled B in figure 2. The movement of this defect can be represented by successive jumps of hexagon vertices, thereby changing the relative orientation of two adjacent rows of hexagons. This leads to two pairs of rows of parallel hexagons

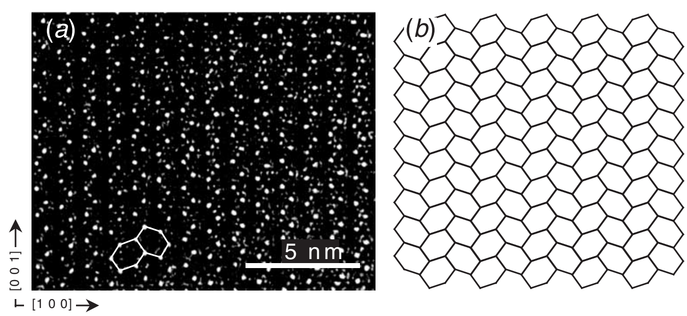

Figure 1. (*a*) Transmission electron micrograph taken along the [010] axis of the perfect ξ′-(Al–Pd–Mn) phase. A bright-dot contrast is observed on the vertices of flattened hexagons with alternating orientations. (*b*) Schematic representation of the perfect ξ′-(Al–Pd–Mn) phase in terms of flattened hexagons arranged in alternating orientations.

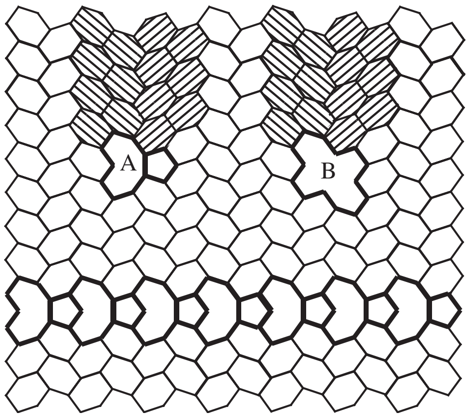

Figure 2. Tiling of flattened hexagons with structural defects. A banana-shaped polygon and an attached pentagon (labelled A) correspond to a phason line with the line direction parallel to [010]. A phason line including a kink (labelled B) in the defect line results in an elongation of the defect along [001]. Both defects have moved from the top part of the tiling to their present positions. In their wake, two rows of hexagons have flipped their orientation, resulting in two pairs of rows of parallel hexagons for each defect (shaded).

along the direction of motion of the defect. In figure 2, showing a downward movement of the defects A and B, the pairs of parallel rows (shaded) are located above the corresponding defects. Physically, the motion of these defects involves atomic jumps (Beraha *et al.* 1997), which lead to a local rearrangement of the structural building blocks while leaving the structure unchanged at large distances. Beraha *et al.* (1997) have shown that the local atomic displacements, similarly to phason defects in quasicrystals, can be described in terms of complementary-space strain fields. Therefore these defects have been referred to as phason defects. In the following we shall term these *phason lines* in order to emphasize their linear character.

It has been shown in a geometrical model that the motion of a great number of phason lines can result in a shape change, that is a plastic shear deformation of the sample (Klein *et al.* 1996). Simultaneously, the sample undergoes a structural change that can eventually lead to an arrangement of flattened hexagons, which are all parallel to each other. A phase with a structure characterized by such an arrangement of flattened hexagons has also been observed in the Al–Pd–Mn alloy system and was termed ξ-(Al–Pd–Mn) (Audier *et al.* 1993).

The introduction of phason lines by plastic deformation has been confirmed experimentally (Klein *et al.* 1996, 2000). Phason lines were reported to be arranged closely neighboured along the [100] direction, leading to the formation of planes perpendicular to the [001] direction as shown in the lower part of figure 2. In the following we shall refer to these planes of phason lines as *phason planes*.

If a high density of phason planes is present in the structure, they can eventually become stacked periodically, forming different superstructures of ξ'-(Al–Pd–Mn) with equal a and b cell parameters, but larger cell parameters along the c direction. A superstructure with a simple rectangular lattice and $c = 44.9$ Å has been observed by Klein (1997). A centred rectangular lattice with $c = 57.0$ Å, referred to as Ψ-(Al–Pd–Mn), has been reported by Klein *et al.* (1999). Other superstructures with $c = 32.4$ Å and $c = 70.1$ Å have been identified by Yurechko *et al.* (2002).

§4. Dislocations

All dislocations presented have line directions parallel to [010] and various Burgers vectors. Note that the orientations of all the figures in this paper, except for figures 11 (*a*) and 12, are identical and correspond to the orientation of the ξ' phase shown in figure 1.

4.1. *Burgers vectors parallel to [001]*

Let us firstly recall some of the results reported by Klein *et al.* (1999). Subsequently, we shall present a generalization of the description and apply it to dislocations with different Burgers vector magnitudes. The dislocation shown in figure 3, even though of a complex structure, is suitable for such an introduction since its line direction is strictly parallel to the observation direction. This facilitates the comparison of the observed structure with its description in terms of a tiling.

Figure 3 (*a*) shows a TEM image of a pure edge dislocation in end-on orientation. The line direction is parallel to [010]. If the vicinity of the dislocation core is covered with a tiling of flattened hexagons, an additional polygon has to be introduced. The boxed area containing the dislocation core is shown magnified in figure 3 (*b*) with the new polygon superimposed. The Burgers vector of this dislocation was determined by high-resolution TEM and contrast extinction experiments (Klein *et al.* 1999) as $(2\tau - 3)d$ [001], where the irrational number $\tau = (1 + 5^{1/2})/2$ is the golden mean and $d = 7.76$ Å is the edge length of the tiles (Beraha *et al.* 1997). This corresponds to a Burgers vector magnitude of 1.83 Å. This dislocation in the ξ' lattice will in the following be referred to as a *lattice dislocation*.

In order to introduce the new polygon characterizing the lattice dislocation into the tiling, three rows of parallel hexagons on one side and five rows of parallel hexagons on the other side of the dislocation core are required. These are shown shaded in figure 3 (*c*). As shown above, the introduction of a phason line changes the relative orientation of two rows of flattened hexagons. Therefore, in the vicinity of the dislocation core, a well-adjusted arrangement of phason lines can accommodate the parallel rows of hexagons to the lattice. In the present case the ideal ξ' structure, as represented by alternatingly oriented flattened hexagons, can be restored at the top and the bottom of figure 3 (*d*) by introducing six phason half-planes. Then the tiling can be continued above and below the phason half-planes by either the perfect ξ' structure or a periodic arrangement of phason lines. In other words, the lattice dislocation can be accommodated into the ξ' structure by decoration with an appropriate defect arrangement on the larger scale of the hexagon tiling.

If the lattice dislocation and the inserted phason half-planes are embedded into a periodic arrangement of phason lines, for example into Ψ-(Al–Pd–Mn), a dislocation-like structure in the phason-line lattice with six inserted phason half-planes results. This corresponds to the situation shown in figure 3 (*a*). Since here the complete structure represents a defect within a defect lattice it has been termed a metadislocation (Klein *et al.* 1999).

We have furthermore observed lattice dislocations, which are accommodated to the crystal lattice by the introduction of four, ten or 16 phason half-planes. Figure 4 (*a*) shows the case for ten half-planes. A still different polygon (figure 4 (*b*)) corresponds to the core of this lattice dislocation (indicated by the white arrow in figure 4 (*a*)). Analogously to the preceding case, this polygon can be brought into registry with the tiling of flattened hexagons by the introduction of suitable numbers of rows of parallel hexagons. In this case, five parallel rows are

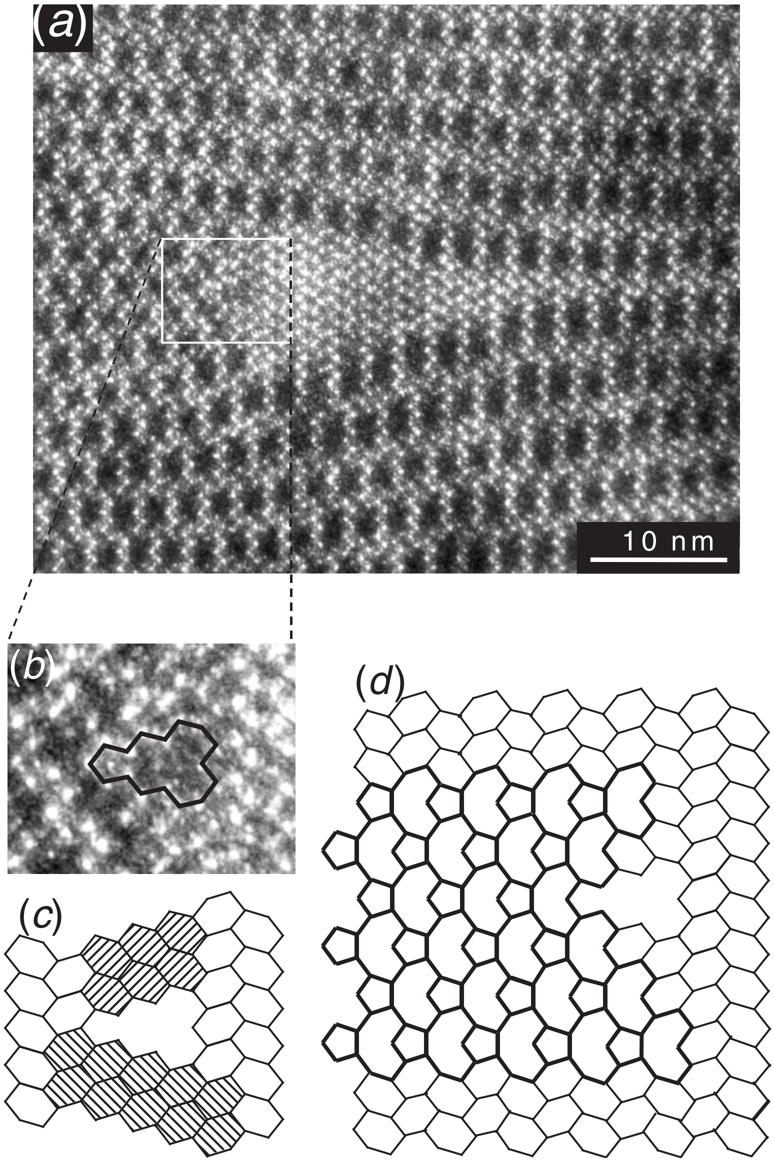

Figure 3. (*a*) Transmission electron micrograph of a metadislocation in the lattice of phason lines taken along the [010] axis. (*b*) Magnification of the boxed region in (*a*) containing the dislocation core with a superimposed new polygon. (*c*) The polygon corresponding to the dislocation core inserted into a tiling of flattened hexagons. The shaded hexagons indicate the rows of parallel hexagons needed to accommodate the lattice dislocation to the tiling of flattened hexagons. (*d*) The insertion of six half-planes of phason lines restores the alternating orientations for the hexagons at the top and the bottom of the figure. In this way the dislocation is brought into registry with the ξ' structure.

necessary on one side and seven parallel rows on the other (shaded in figure 4 (*c*)). The introduction of ten phason half-planes recovers the alternating orientations of the flattened hexagons, that is the ideal ξ' structure (figure 4 (*d*)). Redrawing this polygon using the edge length and angles corresponding to the flattened hexagons

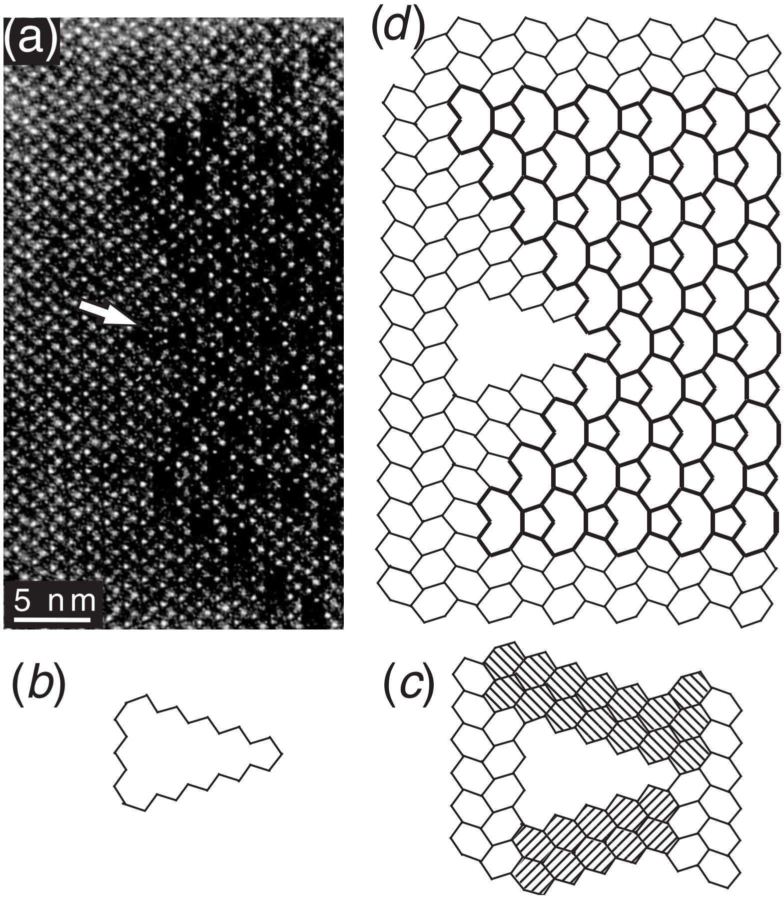

Figure 4. (*a*) Transmission electron micrograph taken along the [010] axis. Ten phason half-planes are attached to a dislocation. The dislocation core is indicated by the white arrow. The unit cell of the ξ' phase and the arrangement of flattened hexagons are indicated in the lower left corner. (*b*) The polygon corresponding to the dislocation core. (*c*) The polygon can be inserted into the tiling of flattened hexagons by introducing five parallel rows of hexagons on one side and seven parallel rows of hexagons (hatched in the figure) on the other side of the dislocation. (*d*) Introducing ten phason half-planes restores the alternating orientations of the flattened hexagons at the top and bottom of the figure.

yields a closure failure corresponding to a Burgers vector of $(5-3\tau)d$ [001]. This corresponds to a magnitude of 1.13 Å, which is smaller by a factor of τ than that in the preceding case.

Figure 5 shows a lattice dislocation connected to 16 phason half-planes. At the core of the dislocation a polygon can be defined (figure 5 (*b*)) that can be inserted in perfect registry with the tiling of flattened hexagons by means of eight rows of parallel hexagons on one side and ten rows of parallel hexagons on the other side of the polygon (shaded in figure 5 (*c*)). 16 half-planes of phason lines are necessary to accommodate this defect into the ξ' structure (figure 5 (*d*)). Redrawing this polygon using the edge length and angles corresponding to the flattened hexagons yields

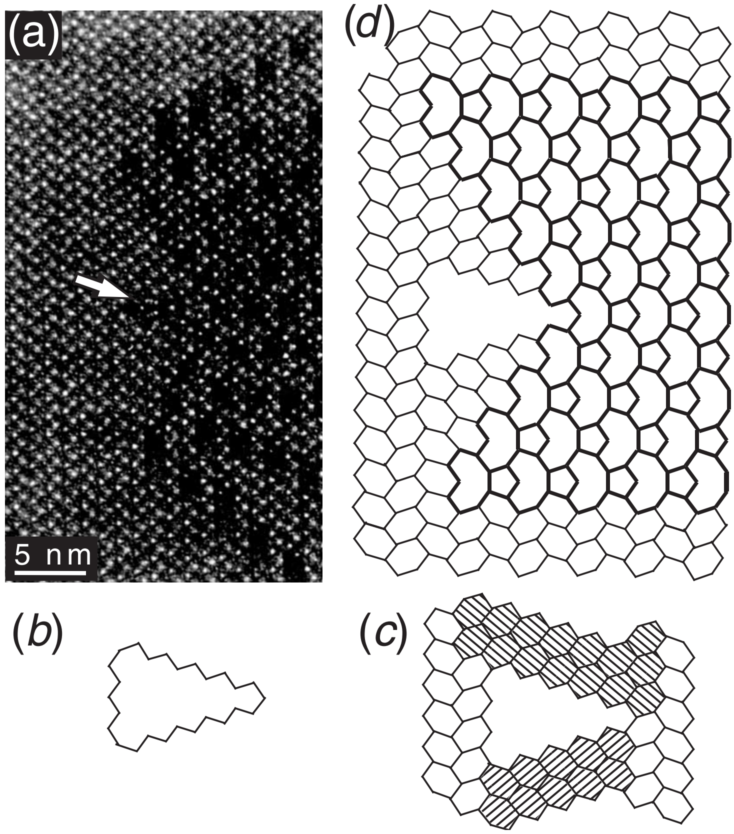

Figure 5. (*a*) Transmission electron micrograph of a dislocation connected to 16 half-planes of phason lines. The dislocation core is indicated by the white arrow. (*b*) The polygon corresponding to the dislocation core. (*c*) The polygon can be inserted into a tiling of flattened hexagons by means of eight and ten rows of parallel hexagons (shaded in the figure) on its two sides. (*d*) The introduction of 16 phason half-planes restores the alternating tiling of the flattened hexagons at the top and bottom of the figure.

a Burgers vector of $(5\tau-8)d$ [001]. This corresponds to a magnitude of 0.70 Å, which is smaller by a factor of τ^2 than that in the first case.

Figure 6 shows a lattice dislocation connected to four phason half-planes. In this case the half-planes are not perpendicular to the [001] direction. They are tilted as indicated by the white lines superimposed on the tiling. The polygon defining the lattice dislocation core (white lines and indicated by a white arrow) is accommodated to the tiling of hexagons by two rows of parallel hexagons on one side and four rows on the other side. Four half-planes of phason lines bring this arrangement into registry with the tiling of alternating orientations of flattened hexagons. Redrawing this polygon using the edge length and angles corresponding to the flattened hexagons yields a Burgers vector of $(\tau-2)d$ [001], that is of magnitude 2.96 Å. This value is larger by a factor of τ than that for the first case.

The characteristics of the dislocations presented in this section are summarized in table 1.

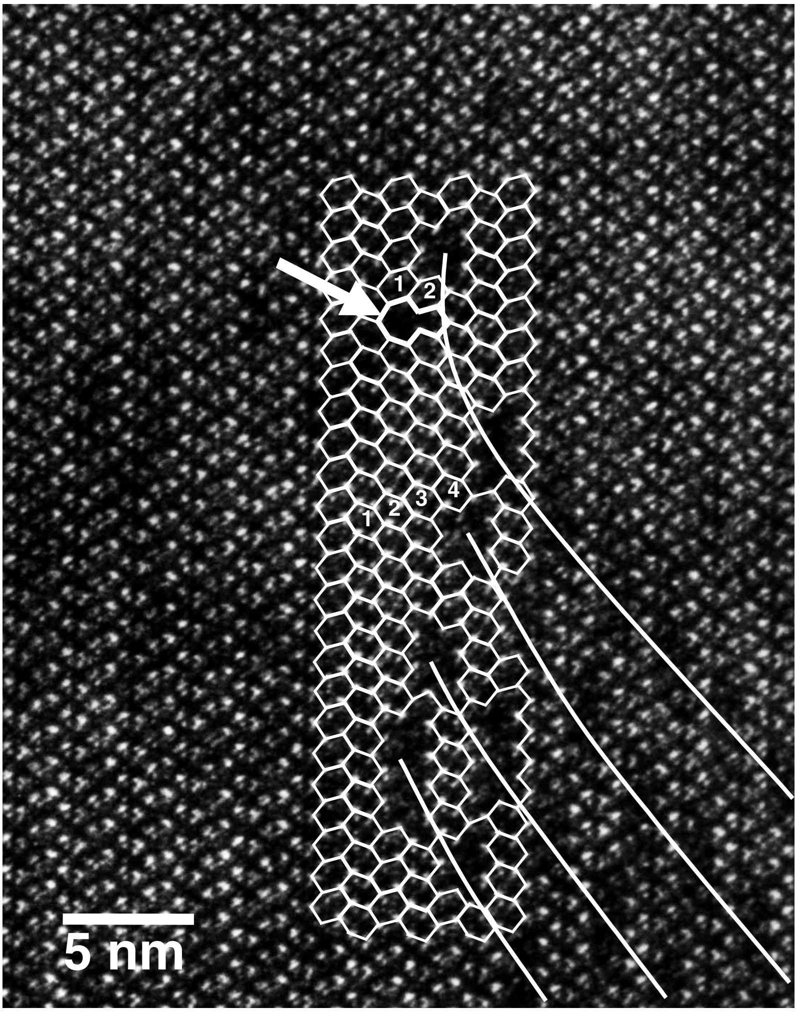

Figure 6. Transmission electron micrograph of a dislocation connected to four half-planes of phason lines. The phason half-planes are inclined as indicated by the white lines superimposed on the image. The dislocation core, indicated by the white arrow, is inserted into the tiling of hexagons by two rows of parallel hexagons on one side and four rows of parallel hexagons on the other.

Table 1. Characteristics of the dislocations with Burgers vectors parallel to [001] observed in the ξ' phase. $\tau = (1 + 5^{1/2})/2$ is the golden mean.

Burgers vector magnitude (Å)	Fraction of the cell parameter c	Number of phason half-planes
2.96	τ^{-3}	$4 = 2 \times 2$
1.83	τ^{-4}	$6 = 2 \times 3$
1.13	τ^{-5}	$10 = 2 \times 5$
0.70	τ^{-6}	$16 = 2 \times 8$

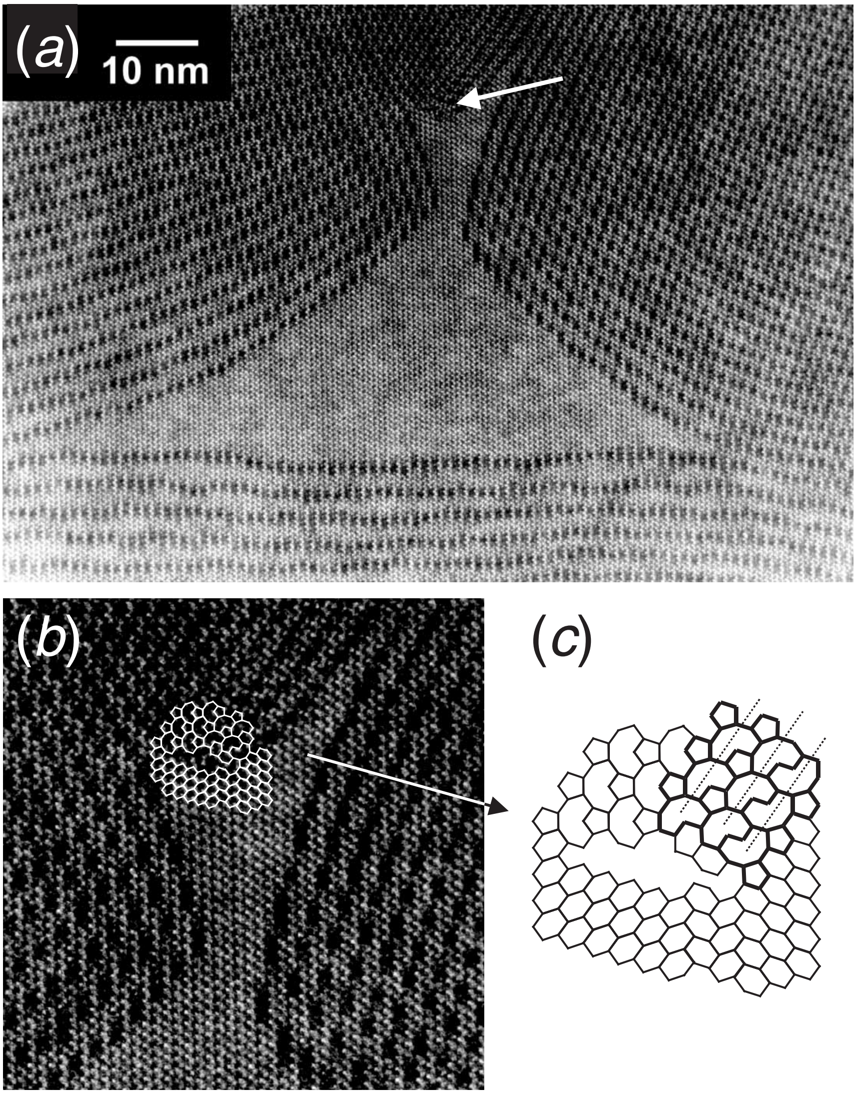

Figure 7. Transmission electron micrograph of a dislocation with a line direction parallel to [010] in the phason-line lattice. In the bottom part of the sack-shaped area free of phason lines the perfect ξ' structure is observed. In the top part, one observes parallel hexagons constituting two twins of the ξ structure. The dislocation core is situated at the top of the area free of phason lines (indicated by the white arrow). (*b*) Enlargement of the zone outlined in (*a*) containing the dislocation core. A tiling of flattened hexagons and phason lines has been superimposed on the region of the dislocation core, revealing its very complex polygon. (*c*) In the extended tiling around the dislocation core, three rows of phason lines rotated by 72° and ending at the dislocation core can be observed. They are indicated by dotted lines.

4.2. *Burgers vectors parallel to [τ01]*

Figure 7 (*a*) shows a lattice dislocation forming a sack-shaped defect structure in the phason-line lattice. The bottom part of the defect structure is made up by the alternating flattened hexagons corresponding to the ideal ξ' structure. In the upper part, one observes two areas of flattened hexagons arranged in parallel corresponding to two twins of the ξ structure. The core of the lattice dislocation is situated at the very top of the defect structure, indicated by the white arrow. Figure 7 (*b*) shows a magnification of the region containing the dislocation core. A tiling is superimposed on the image, featuring a complex new polygon corresponding to the dislocation core. The drawing in figure 7 (*c*) shows the enlarged tiling. Redrawing this polygon using the edge length and angles corresponding to the flattened hexagons yields a Burgers vector of magnitude 1.83 Å. Its direction is turned by 72° from the [001] direction. In terms of the ξ' unit cell this direction can be indexed as [τ01].

From the lattice dislocation core a planar defect extends to the upper right (figure 7 (*c*)). Its structure can be described by three rows of banana-shaped polygons attached to regular pentagons. These are the same polygons as those characteristic of the phason lines described above. In contrast with the latter, however, the long direction of the banana-shaped polygon is in this case not parallel to [001], but turned by 72°.

Figure 8 shows another example of a lattice dislocation, indicated by the white arrow, with a Burgers vector parallel to the [τ01] direction. For this case a Burgers vector of magnitude 2.96 Å, that is larger by a factor of τ than the preceding value, is obtained. Here only two rows of rotated phason lines are observed to end at the dislocation core. Note that the phason lines surrounding the dislocation contain one or several kinks. The corresponding polygons in figure 8 are therefore elongated along [001] in the same way as that labelled B in figure 2.

The characteristics of the dislocations presented in this section are summarized in table 2.

§5. Stacking faults

Stacking faults with two different displacement vectors have been observed in the ξ'-(Al–Pd–Mn) phase. Figure 9 shows a stacking fault where the displacement between the crystalline regions on both sides can be characterized by two back-to-back pentagons (white lines in figure 9). This yields a displacement vector $0.5\tau^{-2}(\tau\, 0 - 1)$. Its magnitude is 7.76 Å and its direction is rotated by 108° with respect to the [001] direction. This corresponds to one of the edges of the pentagons and of the flattened hexagons.

The second type of stacking fault observed is characterized by a more complicated geometry (figure 10). Here the lattices on the two sides of the stacking fault can be linked by a flattened hexagon with edge lengths being τ times larger than those characteristic of the ξ' phase. The resulting displacement vector is $0.5\tau^{-2}(-\tau\, 0 - 1)$. Its magnitude is also 7.76 Å and its direction makes an angle of $-108°$ with the [001] direction. This corresponds to another edge of the flattened hexagons.

§6. Connected dislocations

We have observed dislocations in ξ'-(Al–Pd–Mn) which are mutually connected via their phason half-planes. Figure 11 shows the different types of connection. Three $(2\tau{-}3)d[001]$ dislocations (six phason half-planes) in an otherwise ideal ξ' structure can be observed in figure 11 (*a*). They share some of their phason half-planes. Figure 11 (*b*) shows two $(5{-}3\tau)d[001]$ dislocations (ten phason half-planes) of opposite sign in a periodic array of phason lines. Here the phason half-planes do not link the dislocations but stretch out in opposite directions. In figure 11 (*c*) a $(5{-}3\tau)d[001]$ dislocation is closely connected to a $(2\tau{-}3)d[001]$ dislocation.

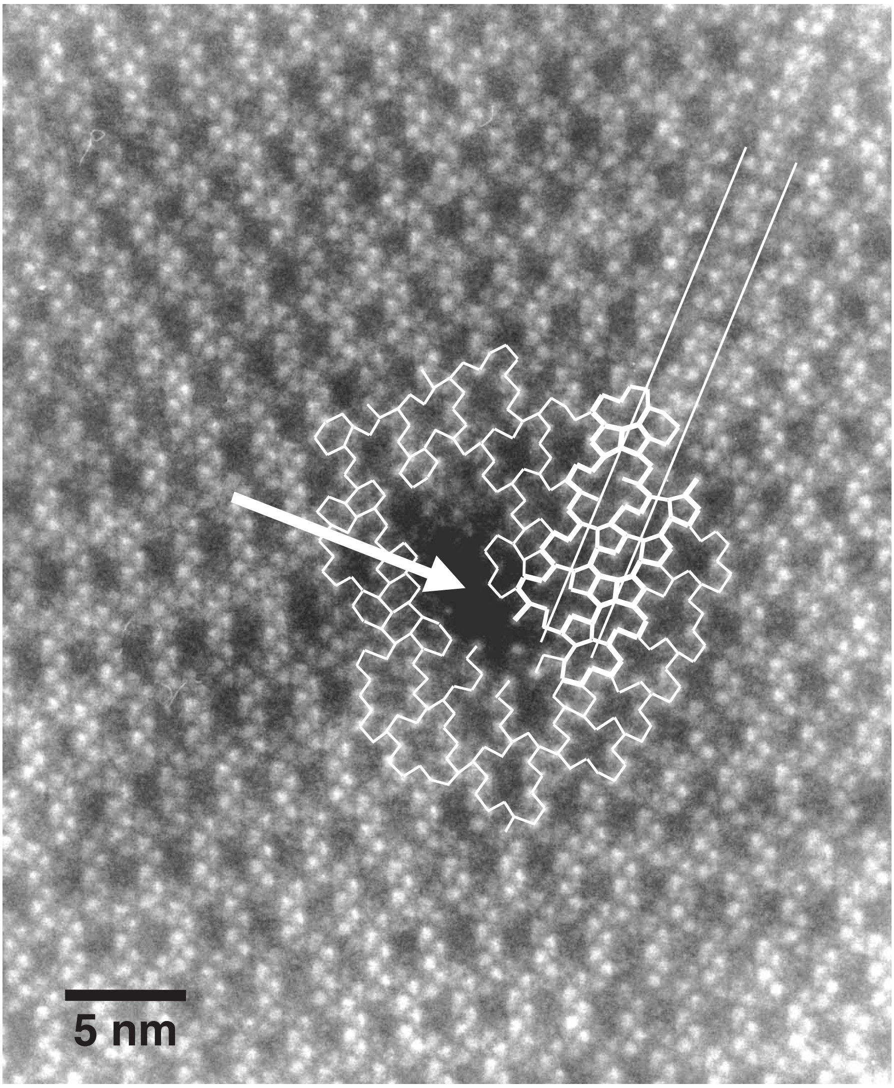

Figure 8. Transmission electron micrograph of a dislocation with a Burgers vector parallel to [τ01] and with a magnitude of 2.96 Å. The dislocation core is indicated by the white arrow. The two white lines superimposed on the image show the two rows of rotated phason lines, which end at the dislocation core.

Table 2. Characteristics of the Burgers vectors parallel to [τ01] observed in the ξ' phase.

Burgers vector magnitude (Å)	Fraction of the cell parameter c	Number of phason half-planes
2.96	τ^{-3}	2 turned by 72°
1.83	τ^{-4}	3 turned by 72°

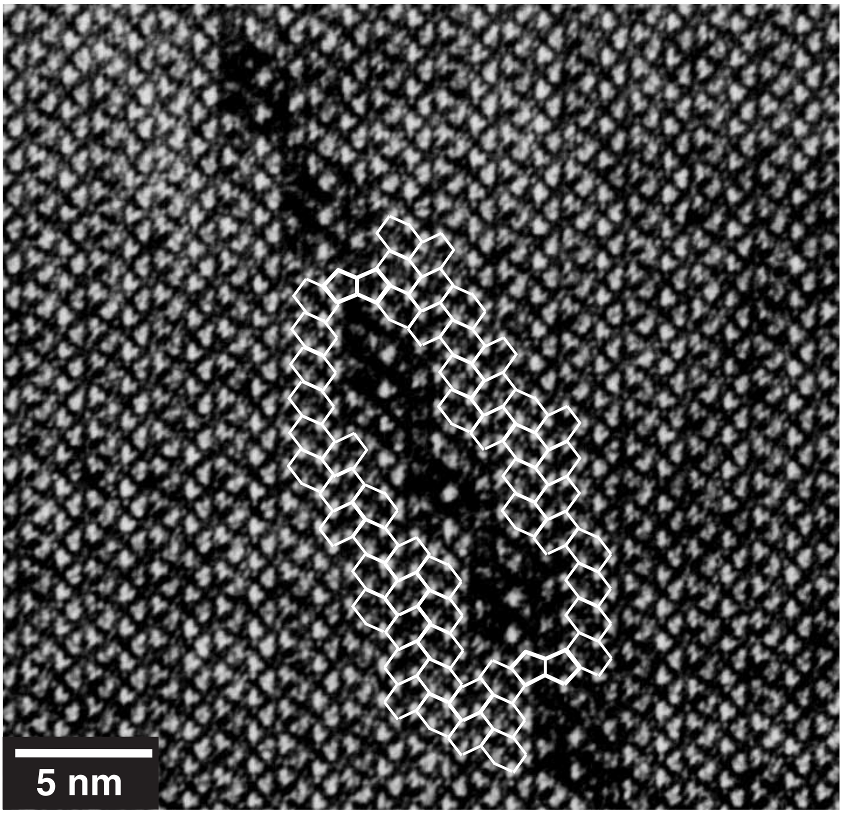

Figure 9. Transmission electron micrograph of a stacking fault in the ξ' phase. Two back-to-back pentagons connect the two halves of the crystal.

They share the six phason half-planes of the latter. Hence only four phason half-planes extend far from this pair of dislocations.

§ 7. Discussion

ξ'-(Al–Pd–Mn) is a complex intermetallic phase, the smallest cell parameter of which, amounts to $c = 12.339$ Å. A perfect dislocation in this structure would have a Burgers vector magnitude of at least this value. Since the elastic line energy of a dislocation is proportional to the square of the magnitude of the Burgers vector (Hirth and Lothe 1968), this would involve unfavourably high line energies. Therefore, our observation that only partial dislocations seem to exist in this material is not surprising. However, we find a number of distinct differences from partial dislocations observed in simple intermetallics.

(i) The magnitudes of the Burgers vectors observed in the ξ' phase are not simple but *irrational* fractions of the cell parameters. They follow a geometrical series linked by factors of τ between subsequent values.

(ii) The accommodation of the [001] partials into the structure of the ξ' phase does *not* involve the introduction of stacking faults. The local changes in the tiling of flattened hexagons caused by the dislocation are compensated by the arrangement of phason lines. In this way, the defect structure accommodates to the perfect ξ' structure and the dislocation acts as a perfect

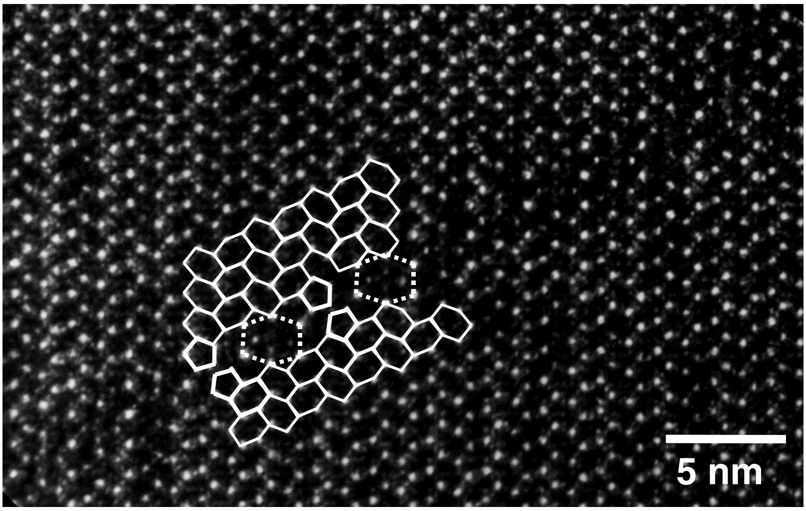

Figure 10. Transmission electron micrograph of a stacking fault in the ξ' phase. The two halves of the crystal are connected by a flattened hexagon (white broken lines) τ times larger than that of the ξ' structure.

dislocation. Accordingly, moving [001] partials in ξ'-(Al–Pd–Mn) do not create stacking faults in their wake.

(iii) The Burgers vector directions of lattice dislocations in ξ'-(Al–Pd–Mn) are not necessarily perpendicular to lattice planes. This is demonstrated in the case of the dislocations shown in figures 7 and 8. Their direction with respect to the ξ' unit cell can be indexed as [τ01], where the golden mean τ is an irrational number.

These features cannot straightforwardly be understood taking into account only the characteristics of the ξ' structure. A comparison with the icosahedral quasicrystal in the Al–Pd–Mn system proves very helpful.

The orientation relationships described in § 3 show that the Burgers vector direction parallel to [001] of the ξ' phase is equivalent to a twofold axis of icosahedral Al–Pd–Mn (Klein *et al.* 1996). In the latter material, the most frequently observed Burgers vector direction is indeed parallel to twofold axes (Rosenfeld *et al.* 1995, Feuerbacher *et al.* 1997). Moreover, the magnitudes of the Burgers vectors in the ξ' phase are identical with the physical-space components of the Burgers vectors in the quasicrystal (table 3). For the latter, the scaling of the Burgers vector magnitudes by factors of τ can be understood regarding the characteristics of the quasicrystal structure, where atomic planes are stacked quasiperiodically, involving two different distances with a ratio of τ. The two distances follow a Fibonacci sequence, which in itself exhibits a τ-scaling behaviour (Janot 1992).

The occurrence of the [τ01] Burgers vector direction in ξ'-(Al–Pd–Mn) can also be conceived by comparison with the quasicrystal. According to the orientation relationships (Klein *et al.* 1996), the [010] axis of the ξ' structure, which is the direction of view in all micrographs shown, is parallel to a fivefold axis of icosahedral Al–Pd–Mn. A rotation of $2\pi/5$ (i.e. 72°) around the latter links two equivalent directions. Hence, the [τ01] direction, which is turned by 72° from the twofold

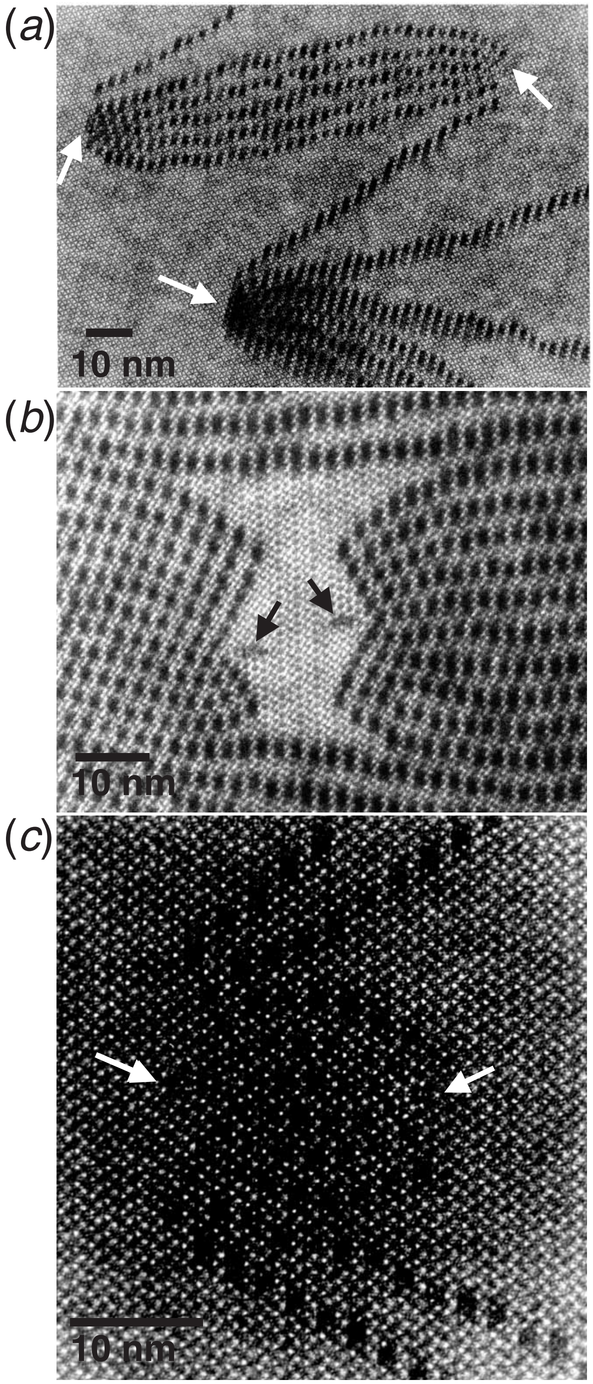

Figure 11. Interactions between metadislocations. The dislocation cores are indicated by white arrows in (*a*) and (*c*) and by black arrows in (*b*). (*a*) Three $(2\tau-3)d$ [001] metadislocations sharing some of their phason half-planes. (*b*) Two 'face-to-face' $(5-3\tau)d$ [001] metadislocations. No phason half-planes are shared. (*c*) A metadislocation connected to ten and one connected to six phason half-planes share six phason half-planes. Four phason half-planes extend far from the dislocations.

Table 3. Comparison of the Burgers vectors observed in the ξ' phase and the Burgers vectors parallel to a twofold axis in the icosahedral phase. Note that both directions [001] and [τ01] in ξ'-(Al–Pd–Mn) are equivalent to a twofold direction in the icosahedral phase. $b_{\parallel}$ and $b_{\perp}$ are the magnitudes of the phonon and phason parts respectively of the 6D Burgers vectors.

ξ'-(Al–Pd–Mn)			Icosahedral Al–Pd–Mn	
Burgers vector magnitude (Å)	Burgers vector direction	Number of phason half-planes	$b_{\parallel}$ (Å)	Phason component of the Burgers vector $b_{\perp}$(Å)
2.96	[001]	$4 = 2 \times 2$	2.96	12.5
1.83	[001]	$6 = 2 \times 3$	1.83	$20.3 = \tau \times 12.5$
1.13	[001]	$10 = 2 \times 5$	1.13	$32.8 = \tau \times 20.3$
0.70	[001]	$16 = 2 \times 8$	0.70	$53.1 = \tau \times 32.8$
2.96	[τ01]	2 (turned by 72°)	2.96	12.5
1.83	[τ01]	3 (turned by 72°)	1.83	$20.3 = \tau \times 12.5$

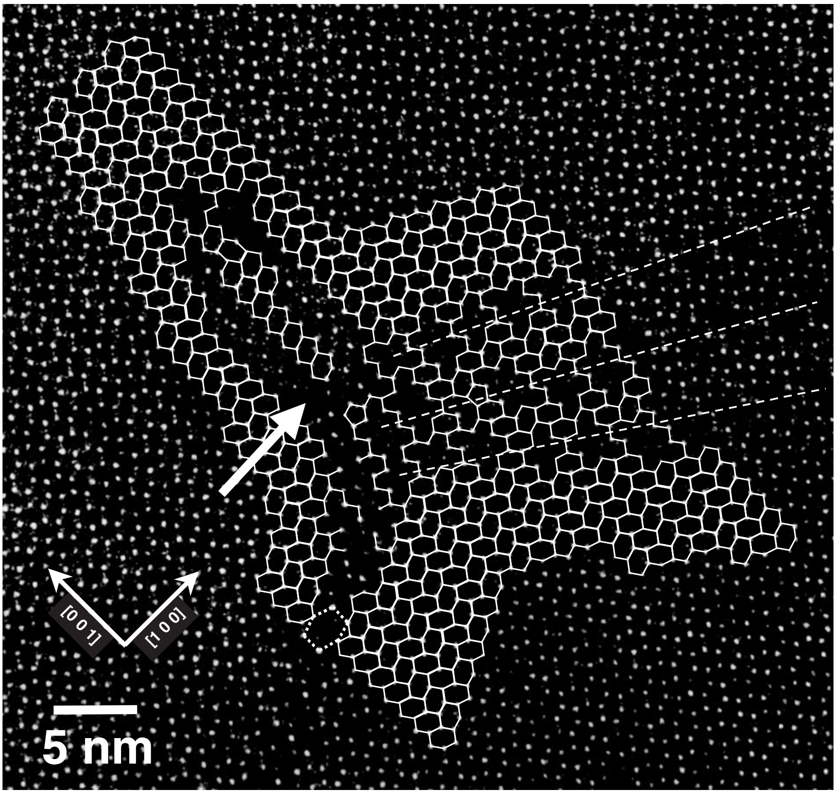

Figure 12. Transmission electron micrograph of a dislocation and a stacking fault. The dislocation core is indicated by a white arrow. In addition to the stacking fault extending downwards, three phason half-planes extend to the right-hand end at the dislocation core.

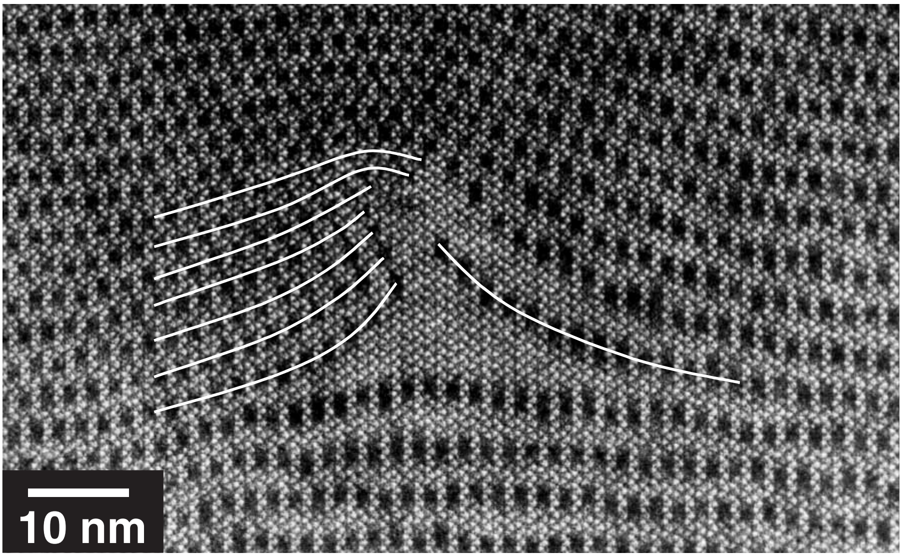

Figure 13. Metadislocation with one phason half-plane pointing towards the dislocation core. This situation can be interpreted as a snapshot of a dislocation moving within the periodic phason-line lattice (see text).

[001] direction of ξ' is also parallel to a twofold axis of the quasicrystal. Therefore, the [τ01] Burgers vector in ξ'-(Al–Pd–Mn) can again be understood to correspond to a twofold Burgers vector in the icosahedral phase. The two different magnitudes of the [τ01] Burgers vector observed are indeed identical with the magnitudes found for parallel-space components of twofold Burgers vectors in icosahedral Al–Pd–Mn (table 3).

The comparison of the dislocations in ξ'-(Al–Pd–Mn) and icosahedral Al–Pd–Mn can be driven even further. Dislocations in the quasicrystal, which have to be described in terms of the 6D hyperlattice, have, in addition to their physical-space Burgers vector component, a component in perpendicular space, the phason component. The latter also shows a τ scaling, which is opposed to that of the physical-space component; when the physical-space component increases by a factor of τ, the phason component decreases by a factor of τ. In the ξ' phase, a similar sequence can be observed if the numbers of phason half-planes of the different dislocations are considered. The number of phason half-planes is always even. This is a consequence of the fact that phason lines occupy alternating positions in neighbouring phason planes. The decreasing series of Burgers vector magnitudes of 2.96 Å, 1.83 Å, 1.13 Å and 0.70 Å is linked to increasing numbers of phason half-planes: 2×2, 2×3, 2×5 and 2×8 respectively (table 3) corresponding to twice the consecutive numbers of the Fibonacci sequence 2, 3, 5 and 8. The ratio of these subsequent numbers approximates the number τ. Thus, we can conclude that the phason half-planes associated with the dislocations in the ξ' phase represent the phason component of their corresponding dislocations in icosahedral Al–Pd–Mn.

These very close relationships between the dislocations in the icosahedral and the ξ' phase show that a dislocation in the latter is sensitive to the local atomic order, which is the feature these phases have in common. The structures of ξ'-(Al–Pd–Mn) and icosahedral Al–Pd–Mn are both based on Mackay-type clusters, which have a diameter of 9.6 Å and local icosahedral symmetry (Janot 1996). Thus, the local order in these two phases is similar on a length scale of, say, 10 Å, which is much larger than the magnitudes of the Burgers vectors. We can therefore conclude that dislocations are primarily sensitive to short-range order and not to long-range periodicity or quasiperiodicity.

The same kind of remark holds also for the stacking faults that we have observed. The displacement vectors have magnitudes and directions that are irrational with respect to the lattice of the ξ' phase. They do correspond, however, to the vectors connecting neighbouring Mackay-type clusters.

One of the dislocations observed does not fit into the above scheme (figure 12). It is connected with three phason half-planes and a stacking fault and has a [001] Burgers vector of magnitude 1.48 Å. No corresponding Burgers vector has been observed in icosahedral Al–Pd–Mn. Regarding the fact that this magnitude is exactly one half of 2.96 Å the following interpretation is possible. This dislocation is the result of the splitting of a $(\tau-2)d[001]$ into two partials. Accordingly, it is connected to a stacking fault, which at its other end should be connected to another partial, not seen in the figure. Note that here the term 'partial' is used in its ordinary sense.

A question arising with defects of such complex structure is the possibility of their movement. Even though the significant increase in the densities of phason lines and dislocations during plastic deformation (Klein *et al.* 2000, Feuerbacher *et al.* 2001) can be interpreted as an indication that these defects mediate plastic deformation, which premises that they are mobile, we do not have any direct insight into the mechanism of their motion. Nevertheless, some clues can be found in the images presented. At the onset of plastic deformation, when the density of phason lines is very low, the motion of a dislocation necessarily has to be accompanied by the motion of the associated phason half-planes. Figure 6 can be interpreted in this sense. Here a dislocation moves upwards, dragging the associated phason half-planes with it. Once the sample has reached a state of high density of phason lines, dislocations have another possibility to move through the crystal. Figure 13 shows a metadislocation with seven attached phason half-planes on one side and another phason half-plane on the other side, pointing towards the dislocation core. This situation can be interpreted as a snapshot of a metadislocation with a 1.83 Å Burgers vector length, that is with six phason half-planes, moving within the lattice of phason lines as an ordinary dislocation does in the lattice of a crystal. A phason plane breaks in front of the metadislocation; one half flips over to the rear of the dislocation and recombines with another phason half-plane. In this way, in complete analogy to the motion of a perfect dislocation in a simple crystal, the metadislocation can move through a periodic lattice of phason lines without the necessity of moving phason half-planes.

A mechanism of this kind should lead to a change in the favourable Burgers vector magnitudes in different stages of plastic deformation. In an early stage, dislocations with a small number of attached phason half-planes should be favoured since, firstly, this minimizes the energy necessary to create the phason-line defects and, secondly, the number of half-planes dragged along with the dislocation is smaller. In later stages, when the structure is enriched with phason lines, dislocations with a smaller Burgers vector magnitude should be favoured owing to their lower elastic line energy. Correspondingly, in the course of plastic deformation a change from larger to smaller Burgers vector magnitudes is expected for the active dislocations. An evolution of this kind has been reported for the case of icosahedral Al–Pd–

Mn (Rosenfeld *et al.* 1995, Feuerbacher *et al.* 1997). In that material, a decrease in the magnitude of the phonon component with increasing plastic strain was found.

Dislocations connected via the associated phason half-planes are shown in figure 11. In figure 11 (*a*), three dislocations with Burgers vector magnitude 1.83 Å, sharing some of their phason half-planes, are shown. Note that the Burgers vector of the dislocation on the right has the opposite sign to those of the dislocations on the left. Subjected to an applied stress, these dislocations would move in opposite directions, which, however, is impeded by the shared phason half-planes. Therefore this association has to be regarded highly immobile. Since phason planes connecting dislocations considerably influence their mobility, the presence of interconnecting phason half-planes can be interpreted as indications of dislocation interactions. In figure 11 (*b*) the dislocations also have Burgers vectors of opposite signs, but they do not share phason half-planes. They should therefore be able to separate and move individually.

In figure 11 (*c*) a still different situation is met. The dislocations with Burgers vector magnitudes of 1.83 Å and 1.13 Å respectively have Burgers vectors of the same sign. The dislocations can move together sharing their six common half-planes of phason lines. In fact, drawing a Burgers circuit around the two dislocations yields a Burgers vector of 2.96 Å. Four phason half-planes stretch out from this dislocation dipole, which indeed is characteristic of a dislocation with a Burgers vector magnitude of 2.96 Å. The dislocation dipole can therefore be regarded as resulting from a dislocation dissociation. A corresponding dislocation reaction in icosahedral Al–Pd–Mn has been observed by Wang *et al.* (1998).

§ 8. Conclusion

In this paper we have reported defects in the complex intermetallic ξ′-(Al–Pd–Mn) phase. The dislocations observed have Burgers vectors, the magnitudes of which are irrational fractions of the unit-cell parameters and whose directions can be incommensurate with respect to the unit cell. This and the high degree of similarity of the lattice dislocations observed in the ξ′-(Al–Pd–Mn) and the icosahedral Al–Pd–Mn phases leads to the conclusion that dislocations are sensitive to the similarities between both phases. These similarities are situated at the level of local atomic order. The dislocations only 'see' this local order and do not 'sense' the long-range periodicity or quasiperiodicity. The distinction of the role of local order as opposed to periodicity was possible in the present work because, in the large unit cell of the ξ′ phase, local order and periodicity do not occur on the same length scales.

References

Audier, M., Durand-Charre, M., and de Boissieu, M., 1993, *Phil. Mag.* B, **68**, 607.

Beraha, L., Duneau, M., Klein, H., and Audier, M., 1997, *Phil. Mag.* A, **76**, 587.

Bohsung, J., and Trebin, H.-R., 1989, *Introduction to the Mathematics of Quasicrystals*, edited by M.V. Jaric (London: Academic Press), p.183.

Boudard, M., de Boissieu, M., Janot, C., Heger, G., Beeli, C., Nissen, H.-U., Vincent, H., Ibberson, R., Audier, M., and Dubois, J.M., 1992, *J. Phys.: condens. Matter*, **4**, 10 149.

Boudard, M., Klein, H., de Boissieu, M., Audier, M., and Vincent, H., 1996, *Phil. Mag.* A, **74**, 939.

Feuerbacher, M., Klein, H., and Urban, K., 2001, *Phil. Mag. Lett.*, **81**, 639.

Feuerbacher, M., Metzmacher, C., Wollgarten, M., Urban, K., Baufeld, B., Bartsch, M., and Messerschmidt, U., 1997, *Mater. Sci. Engng*, **A233**, 103.

Feuerbacher, M., Thomas, C., and Urban, K., 2003, *Single Quasicrystal Growth, in Quasicrystals*, edited by H.-R. Trebin (Berlin: VCH Wiley).
Hirth, J. P., and Lothe, J., 1968, *Theory of Dislocations* (New York: McCraw-Hill).
Janot, C., 1992, *Quasicrystals, A Primer* (Oxford: Clarendon); 1996, *Phys. Rev.* B, **53**, 181.
Klein, H., 1997, PhD Thesis, Institut National Polytechnique de Grenoble, France.
Klein, H., Audier, M., Boudard, M., de Boissieu, M., Beraha, L., and Duneau, M., 1996, *Phil. Mag.* A, **73**, 309.
Klein, H., Feuerbacher, M., Schall, P., and Urban, K., 1999, *Phys. Rev. Lett.*, **82**, 3468; 2000, *Phil. Mag. Lett.*, **80**, 11.
Kléman, M., 1995, *Czech. J. Phys.*, **45**, 11.
Rosenfeld, R., Feuerbacher, M., Baufeld, B., Bartsch, M., Wollgarten, M., Hanke, G., Beyss, M., Messerschmidt, U., and Urban, K., 1995, *Phil. Mag. Lett.*, **72**, 375.
Sauthoff, G., 1995, *Intermetallics* (Weinheim: VCH).
Stadelmann, P. A., 1987, *Ultramicroscopy*, **21**, 131.
Wang, R., Feuerbacher, M., Wollgarten, M., and Urban, K., 1998, *Phil. Mag.* A, **77**, 523.
Wollgarten, M., Beyss, M., Urban, K., Liebertz, H., and Köster, U., 1993, *Phys. Rev. Lett.*, **71**, 549.
Wollgarten, M., Gratias, D., Zhang, Z., and Urban, K., 1991, *Phil. Mag.* A, **64**, 819.
Yamaguchi, M., and Umakoshi, Y., 1990, *Prog. Mater. Sci.*, **34**, 1.
Yurechko, M., Grushko, B., Velikanova, T., and Urban, K., 2002, *J. Alloys Compounds*, **337**, 172.